NeuroImage **17,** 1144–1161 (2002)
doi:10.1006/nimg.2002.1250

# Is It Tonotopy after All?

Marc Schönwiesner,*,†,[1] D. Yves von Cramon,† and Rudolf Rübsamen*

**Faculty of Biosciences, Pharmacy and Psychology, University of Leipzig, and*
*†Max-Planck-Institute of Cognitive Neuroscience, Leipzig, Germany*

Received January 14, 2002

**In this functional MRI study the frequency-dependent localization of acoustically evoked BOLD responses within the human auditory cortex was investigated. A blocked design was employed, consisting of periods of tonal stimulation (random frequency modulations with center frequencies 0.25, 0.5, 4.0, and 8.0 kHz) and resting periods during which only the ambient scanner noise was audible. Multiple frequency-dependent activation sites were reliably demonstrated on the surface of the auditory cortex. The individual gyral pattern of the superior temporal plane (STP), especially the anatomy of Heschl's gyrus (HG), was found to be the major source of interindividual variability. Considering this variability by tracking the frequency responsiveness to the four stimulus frequencies along individual Heschl's gyri yielded medio-lateral gradients of responsiveness to high frequencies medially and low frequencies laterally. It is, however, argued that with regard to the results of electrophysiological and cytoarchitectonical studies in humans and in nonhuman primates, the multiple frequency-dependent activation sites found in the present study as well as in other recent fMRI investigations are no direct indication of tonotopic organization of cytoarchitectonical areas. An alternative interpretation is that the activation sites correspond to different cortical fields, the topological organization of which cannot be resolved with the current spatial resolution of fMRI. In this notion, the detected frequency selectivity of different cortical areas arises from an excess of neurons engaged in the processing of different acoustic features, which are associated with different frequency bands. Differences in the response properties of medial compared to lateral and frontal compared to occipital portions of HG strongly support this notion.** 

## INTRODUCTION

Tonotopy is a general principle of the functional organization of the auditory system. It arises in the sensory epithelium through the structure of the cochlea and is maintained throughout the central auditory pathway by means of orderly projections between auditory nuclei. Details of the tonotopic organization of the auditory cortex in nonhuman primates were revealed by electrophysiological recordings (Merzenich and Brugge, 1973; Imig *et al.*, 1977; Morel and Kaas, 1992; Morel *et al.*, 1993). Cytoarchitectonical studies in both monkeys and humans gave further insight into the anatomical parcellation of respective cortical areas located on the superior temporal plane (STP) (Mesulam and Pandya, 1973; Pandya and Sanides, 1973; Imig *et al.*, 1977; Fitzpatrick and Imig, 1980; Galaburda and Sanides, 1980; Galaburda and Pandya, 1983; Rauschecker, 1997; Rauschecker *et al.*, 1997; Rivier and Clarke, 1997). Subsequently, various attempts were made to align the functional and the anatomical "maps" which, in brief, led to the following widely accepted model: (1) A core region of the auditory cortex, distinguished by a dense granular layer IV (koniocortex), comprises two (Merzenich and Brugge, 1973; Imig *et al.*, 1977; Morel *et al.*, 1993) or three (Morel and Kaas, 1992; Hackett *et al.*, 1998; Kaas and Hackett, 1998, 2000) tonotopic maps with mirror-oriented frequency gradients. The respective maps consist of medio-laterally oriented isofrequency bands which are aligned from occipito-medial to fronto-lateral along the lower bank of the lateral sulcus. It is not known which particular acoustic features, if any, are represented along the auditory cortex perpendicular to the tonotopic gradient. (2) A number of different areas, jointly named the *auditory belt*, surround the core region and embody second level auditory processing. The auditory belt is thought to include seven or more cytoarchitectonically distinct cortical areas, some of which seem to be tonotopically organized as well (Pandya and Sanides, 1973; Kaas and Hackett, 1998; Kaas and Hackett, 2000). These second level areas receive only a sparse thalamic input and depend largely on the input from the core fields (Rauschecker *et al.*, 1997). Electrophysiological recordings gave evidence that neurons of the auditory belt have rather variable response properties and are often best activated by complex combinations of signal features (Rauschecker *et al.*, 1997). (3)

[1] To whom correspondence should be addressed at Faculty of Biosciences, Pharmacy and Psychology, University of Leipzig, Talstrasse 33, 04103 Leipzig, Germany. Fax: +49 341 9736 848. E-mail: marcs@uni-leipzig.de.



1053-8119/02 $35.00

A third level of auditory processing is thought to take place in a region named the *auditory parabelt*, a cortical domain localized laterally to the auditory belt on the dorsal and dorsolateral surface of the superior temporal gyrus (Pandya and Sanides, 1973; Rauschecker *et al.*, 1995, 1997).

In humans, however, the relationship between cytoarchitectonically defined fields of the auditory cortex and physiologically characterized areas is less well established. For obvious reasons, electrophysiological mapping of the cortical tonotopy was rarely performed (Ojemann, 1983; Howard *et al.*, 1996). The available data mostly come from studies which make use of noninvasive imaging techniques such as magnetoencephalography (Romani *et al.*, 1982; Pantev *et al.*, 1988, 1989), positron emission tomography (Lauter *et al.*, 1985; Lockwood *et al.*, 1999), and functional magnetic resonance imaging (Wessinger *et al.*, 1997; Bilecen *et al.*, 1998; Talavage *et al.*, 2000).

Despite the discrepancies in the precise orientation and the number of tonotopic maps proposed in the cited studies, they consistently show that high-frequency-responsive areas are located occipito-medially from low-frequency areas on Heschl's gyrus (HG). These findings are taken as an indication of tonotopical organization of the human auditory cortex, despite (1) the fact that they do not match the complex functional architecture of the auditory cortex in nonhuman primates and (2) the uncertainty of constructing a tonotopic map from only two data points, without probing the progression in between them. The latter difficulty arises from the fact that the bulk of studies employed only two spectrally different stimuli, which are insufficient to probe tonotopic gradients.

Furthermore, the spatial relationship of tonotopic maps from different studies and their orientation with respect to defined cortical landmarks is still subject to debate. Even in the most recent studies there is only little consensus with regard to the functional and anatomical parcellations of the auditory cortex (including the nomenclatures used) (Rivier and Clarke, 1997; Scheich *et al.*, 1998; Hashimoto *et al.*, 2000; Talavage *et al.*, 2000; Morosan *et al.*, 2001).

The present functional MRI study investigates the frequency-dependent localization of acoustically evoked BOLD responses within the human auditory cortex using four spectrally different stimuli. Since nonprimary auditory cortex is better activated by bandpass and modulated signals than by pure tones (Rauschecker, 1997; Wessinger *et al.*, 2001), we used stochastically modulated pure tones with sufficient acoustical complexity to activate primary as well as higher order auditory areas.

By examining the cortical activity pattern in individual subjects, we intended to identify areas with significant frequency-dependent activation in the region of the superior temporal plane and their role with regard to proposed tonotopic maps. In addition, we wanted to study the influence of the individual gyral structure on the activation pattern.

## MATERIAL AND METHODS

### *Subjects*

Thirteen healthy right-handed individuals (six females, seven males) ranging in age from 22 to 27 years were tested on 2 days. The subjects had no history of neurological illnesses and were accustomed to the scanning equipment and procedure. All subjects were right handed as assessed by the Edinburgh Inventory (Oldfield, 1971). The study was approved by the local ethics review board at the University of Leipzig.

### *Acoustic Stimulation and Experimental Design*

In this work, random frequency-modulated sine tones (RFMs) were used for acoustic stimulation. The RFMs consisted of a series of short frequency modulation sweeps with random slope and direction and a total length of 1250 ms. Center frequencies of the four stimuli were 0.25, 0.5, 4.0, and 8.0 kHz, and the respective modulation depth was 20%. The RFM stimuli combine reasonable acoustic complexity with restrictions of the bandwidth necessary to obtain frequency-specific cortical activation patterns. Their stochastic nature only causes a slight widening of the Fourier spectra. Additionally, pure tones with frequencies set at the center frequencies of the RFMs were generated and one subject underwent the experimental procedure twice, with the only difference being the type of acoustic stimuli that were presented: either RFMs or pure tones.

Stimulus frequencies from 0.8 to 3.0 kHz were avoided, since the major part of the sound energy arising from gradient switching lies within that frequency band and could have interfered with the acoustic stimulation.

It has been shown that actively directing the subjects' attention toward a stimulus can lead to increased activity in auditory cortical areas (Woldorff *et al.*, 1993; Grady *et al.*, 1997). In order to increase and control the subject's attention, a simple deviant detection task was utilized in the present study. Half of the presented RFMs contained an additional minute spectral shift, which could be easily perceived as a twitch of the center frequency. These stimuli are in the following referred to as *deviants*. The stimuli without such additional modulations are referred to as *standard stimuli*. With each stimulus the subjects had to decide whether they heard a standard or a deviant stimulus and they had to indicate their decision by pressing one of two buttons.

A common problem of auditory fMRI studies is the hemodynamic interaction between the experimental stimuli and the scanner noise. Several solutions to this

problem have been proposed (low noise image acquisition sequences, Scheich *et al.*, 1998; clustered volume acquisition, Edmister *et al.*, 1999; sparse imaging, Hall *et al.*, 1999). These methods inevitably lead to a reduced number of images acquired in a given period of time. In the present study, a fast EPI sequence was utilized, with image acquisitions clustered at the first 750 ms of a repetition interval of 2 s. During the remaining 1250 ms, the auditory stimuli were presented. Additionally, only a small amount of the sound energy of the scanner noise fell within the frequency bands used for auditory stimulation. These two precautions resulted in a clear separation of stimuli and scanner noise in the time and frequency domain. Contrasting the experimental conditions, which included tonal stimulation and scanner noise, with a baseline condition during which only the ambient scanner noise was audible eliminated the unwanted BOLD response to the scanner noise.

The stimuli were presented in an epoch-related design, where each block was 20 s long and consisted of 10 sequential repetitions of 2 s. Within a single block either acoustic stimuli of one of the four center frequencies (frequency block) or no stimuli (baseline block) were presented. The frequency and baseline blocks were presented in pseudo-randomized order. In order to increase the number of recorded brain volumes per frequency block only 20% of the presented blocks were baseline blocks and consequently not every frequency block was followed by a baseline block. While this design has implications for highpass filtering the fMRI time series (see fMRI Data Acquisition and Analysis), it is irrelevant for statistical modeling. Within the four different frequency blocks (0.25, 0.5, 4.0, and 8.0 kHz) standard stimuli were presented interleaved with the appropriate deviant stimuli in equal proportions and pseudo-randomized order. The frequency and the baseline blocks were repeated 24 times leading to 240 recorded brain volumes under each experimental condition and an overall experimental time of 40 min.

### *Investigational Procedure*

Prior to the functional scanning, the subjects had to read an instruction text on a video display where examples of all acoustic stimuli were presented and the keys to press were indicated. The display was mounted at the face of the gradient coil and was visible to the subjects via mirror goggles. During the experiment, the light was extinguished and the video display was switched off.

The subjects' heads were immobilized with padding on the scanner bed. Pulse and oxygen level were monitored during the experiment. The acoustic stimuli were generated with a PC sound card and presented via electrostatic headphones (Resonance Technology Inc., CA). The earmuffs of the headphones served as passive noise attenuation and reduced the intensity of the imager noise by approximately 25 dB. Clinical earplugs attenuated the scanner noise by another 25 dB. The output adjustments of the sound card were adapted empirically to compensate for the nonlinear filter characteristics of the earplugs.

### *FMRI Data Acquisition and Analysis*

The study was performed at 3 T using a Bruker Medspec 30/100 system (Bruker Medizintechnik, Ettlingen, Germany). A gradient-echo EPI sequence was used with a TE 30 ms, flip angle 90°, TR 2 s, acquisition bandwidth 100 kHz. Acquisition of the slices within the TR was arranged so that the slices were all rapidly acquired followed by a period of no acquisition to complete the TR. The matrix acquired was $64 \times 64$ with a FOV of 19.2 mm, resulting in an in-plane resolution of $3 \times 3$ mm. The slice thickness was 3 mm with an interslice gap of 1 mm. Six horizontal slices parallel to the AC-PC line were scanned. During the same session and prior to the functional scanning, anatomical images were acquired to assist localization of activation foci using a T1-weighted 3-D-segmented MDEFT sequence (Ugurbil *et al.*, 1993) [data matrix $256 \times 256$, TR 1.3 s, TE 10 ms, with a non-slice-selective inversion pulse followed by a single excitation of each slice (Norris, 2000)].

The fMRI time series was analyzed on a single-subject basis using in-house software (Lohmann *et al.*, 2001). Preprocessing of the raw fMRI time series included motion correction using a matching metric based on linear correlation, correction for the temporal offset between the slices acquired in one scan, and removal of low-frequency baseline drift with a temporal highpass filter. The cutoff of the highpass filter was calculated using a standard procedure in fMRI data analysis by determining the maximal time difference between consecutive trial onsets of one condition for each of the conditions and multiplying the minimum of these time differences by two. This procedure ensures that the highpass filter preserves all signal changes induced by the paradigm. Because of the nonalternating experimental design, the cutoff was relatively high (142 time steps) and we checked the individual fMRI raw data for residual baseline effects. No baseline drift could be detected in any dataset after filtering.

The anatomical slices were then coregistered with a full-brain scan that resided in the stereotaxic coordinate system by means of a rigid linear registration with six degrees of freedom (3 rotational, 3 translational). The transformation parameters obtained from this step were subsequently applied to the functional slices so that they were also registered into the stereotaxic space. The statistical evaluation was based on a least-squares estimation using the general linear model for serially autocorrelated observations (Friston *et al.*, 1995a,b; Worsley and Friston, 1995). The design matrix was generated with a boxcar function that in-

cluded a response delay of 6 s. The model equation, including the observation data, the design matrix, and the error term, was temporally smoothed by convolution with a Gaussian kernel of dispersion of 4 s FWHM. No spatial smoothing was performed. The model includes an estimate of temporal autocorrelation that is used to estimate the effective degrees of freedom. Contrasts were calculated between the four frequency conditions and the baseline condition and between the two high-frequency conditions versus the two low-frequency conditions. A *t* statistic was computed from the estimated parameters and the resulting *t* maps were converted to *z* maps (SPM{Z}). The *P* values (uncorrected) pertaining to the *z* scores were used to test anatomically constrained hypotheses about the location of activated areas in individual subjects.

### *Second Level Analysis*

Activated areas that were consistently found in the subjects were identified and named in accordance with the nomenclature introduced by Talavage and co-workers (2000) based on the correspondence of Talairach coordinates of respective activation sites reported in both studies. The nomenclature was slightly expanded to accommodate all activated areas found in the present study. Mean locations of activation foci were computed by averaging the locations of respective local maxima in the SPM{Z} across subjects.

In order to account for anatomical variations of Heschl's gyrus in different subjects the percentage signal change was traced along the frontal and the occipital wall of the individual HG ("tubular regions of interest"). In each (anatomical) sagittal slice of the subjects, Heschl's gyrus was identified according to the definitions given by Penhune *et al.* (1996) and Leonard *et al.* (1998), and voxels with 45% of the maximal gray value in the data set were marked on the image (Fig. 1C). Subsequently, Talairach coordinates of the frontal-most (highest Talairach *y* coordinate) and the occipital-most (lowest Talairach *y* coordinate) of the marked voxels forming the contour of HG were recorded. For statistical analysis, the distance in Talairach millimeters between the Talairach *y* coordinates of the two voxels was taken as the width of HG on the respective sagittal slice. In the registered functional data sets, the voxels corresponding to the frontal- and occipital-most anatomical voxels of the HG contour were obtained. The mean percentage signal change was computed along the frontal and occipital wall of HG respectively by averaging the signal change in these voxels and their eight in-plane neighbors for each sagittal plane. The gradient of the signal change along the walls of HG was then plotted for the four frequency conditions, normalized by linear interpolation to the length of the longest HG in the sample (40 mm), and averaged across subjects. These plots will be referred to as frequency profiles. Computing the differences in percentage signal change between the pooled high- vs the low-frequency conditions yielded gradients of frequency selectivity along the walls of HG.

## RESULTS

### *Anatomical Variability*

Although most of the obtained activation sites were consistent in size and spatial relationship across subjects, there was still a distinct interindividual variability, which had to be considered in analyzing the data. The transverse gyrus of Heschl is known to exhibit a great interindividual anatomical variability, partly because its crown is frequently indented by an intermediate sulcus (SI), causing a partial or complete duplication (bifurcation) of the gyrus (Penhune *et al.*, 1996; Leonard *et al.*, 1998). Three of the 13 subjects studied showed a bifurcation of HG in the left hemisphere and four subjects in the right hemisphere. In two subjects HG was bifurcated on both sides, and the remaining four subjects had nonbifurcated gyri on either side. Taken together, 11 out of 26 HG showed a bifurcation, five in the left and six in the right hemisphere. The bifurcation of HG was most prominent in fronto-lateral aspects of the STP, while the gyri merged toward its occipito-medial border.

For the left hemisphere, Fig. 1 gives a graphical representation of the course of the frontal and occipital walls of HG in terms of Talairach coordinates (Fig. 1A). Both landmarks angle forward in their medio-lateral progression. The distance between the frontal and the occipital wall of HG, projected onto a Talairach *z* plane, was taken as an estimate of the width of HG (Figs. 1B and 1C). The median of the width of HG varied only slightly along the medio-lateral HG extension (Fig. 1B); still the variance of the HG width was higher at its lateral extreme (Talairach $x$ −50 to −47) compared to the medial extreme (Talairach $x$ −35 to −33; $P < 0.05$, Moses rank-like test for scale differences). In order to test if the anatomical variability of the lateral HG is related to the variability of functional activation patterns (described below), subjects were ranked according to the width of their HG between Talairach $x$ −47 and −45 (Fig. 1D). A second ranking was performed according to a parameter of the localization of activated areas, i.e., the distance between two activation foci on (or near) lateral HG (mean Talairach $x$ −47). The two rankings showed a significant correlation (Spearman rank order correlation coefficient $r_s = 0.57$, $P < 0.05$). For illustration, Figs. 2 and 3 show data from two individuals with different anatomies and the respective patterns of activation.

Subject FR1T had a nonbifurcated HG in the left hemisphere with a constant width of about 1 cm (Fig. 1A). Acoustic stimulation with RFM signals limited to defined frequency ranges yielded discrete areas of activation as seen on an axial slice through HG (Fig. 2B;

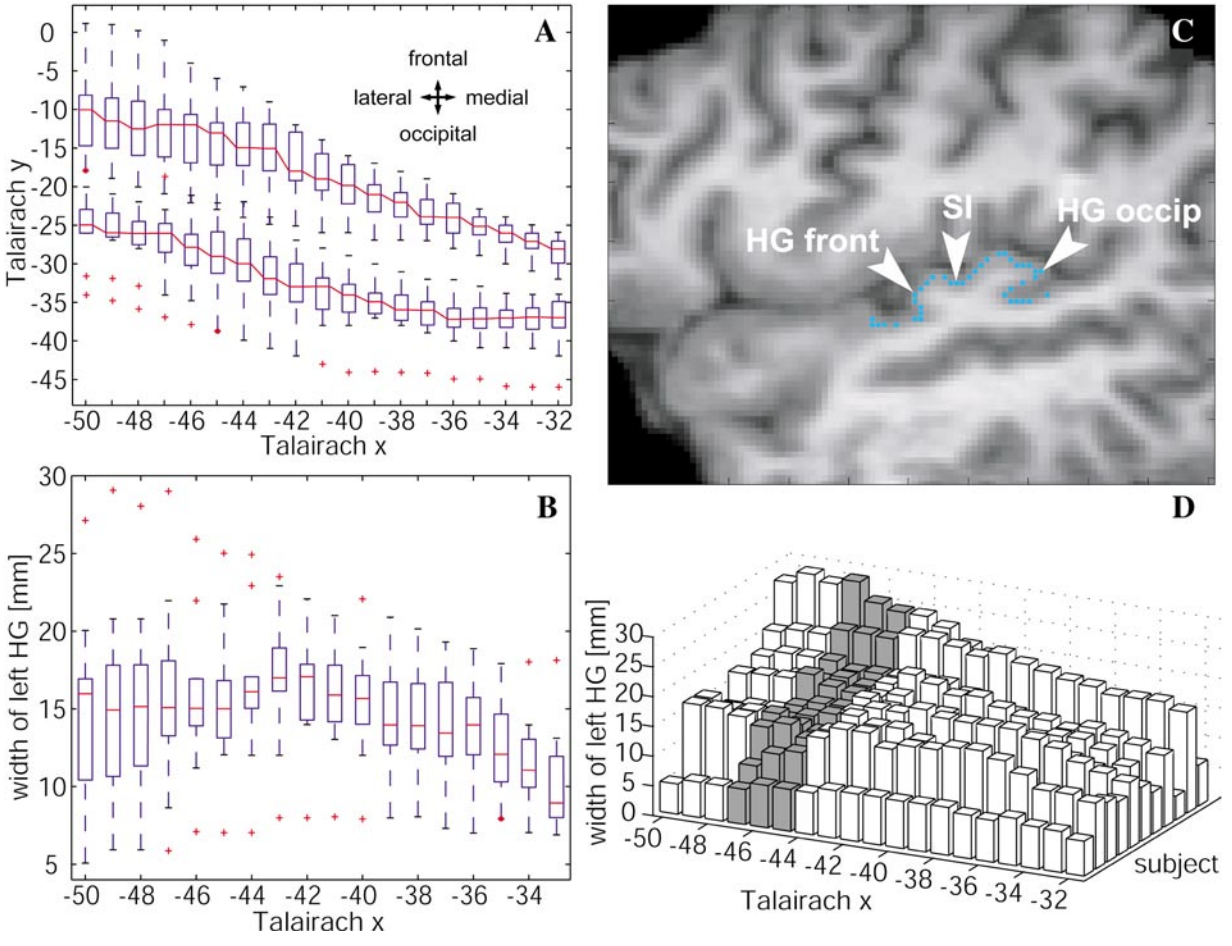


**FIG. 1.** (A) Graphical representation (box and whisker plot; box, median and interquartile range; whiskers, data range; red crosses, outliners) of the average course of the frontal and occipital walls of the left Heschl's gyrus in terms of Talairach coordinates. (B) Graphical representation of the width of the left HG along its medio-lateral extension (box and whisker plot as above). The average width is nearly constant along HG (~15 mm) whereas the variance of the width increased laterally. (C) Illustration of the procedure employed to extract the course of the walls of HG from individual anatomical slices. For each subject, HG was identified and the coordinates of its frontal-most (HG front) and occipital-most (HG occip) voxel on each sagittal slice (between Talairach $x$ −50 and −32) were recorded. The same coordinates were also used for the construction of the individual tubulous regions of interest, along which the fMRI signal was tracked for subsequent analysis. The diameter of these regions was 3 × 3 functional voxels. In the subject shown, the crown of HG is indented by the intermediate sulcus (SI). (D) A ranking of the subjects according to the width of their HG (indicated by bars) between $x$ −47 and −45 (gray bars) was performed. A correlation analysis of this ranking and a second one according to the distance between foci 1a and 1b (mean Talairach $x$ −47) revealed a significant correlation (Spearman rank-order correlation coefficient $r_s = 0.57$, $P < 0.05$). Only the 11 subjects clearly showing both foci were included in the analysis.

a detailed analysis of the frequency-dependent activation will be given below). If high (HF)- and low-frequency (LF) conditions were contrasted (Fig. 2C), two HF foci (marked in blue) appear in proximity to the occipito-medial border of HG and two interconnected LF foci (marked in red) flank the gyrus at more fronto-lateral aspects. The parasagittal slice indicates that the activated LF areas coincide with the superior part of the frontal and occipital wall of HG (Fig. 2D). The present example does not reveal whether the fronto-lateral area of activity represents a single or two separate foci.

In subject SJ2T, an expanded and fronto-laterally bifurcated Heschl's gyrus is seen in the STP-surface reconstruction (Fig. 3A). The distance between the two sulci, which form the respective frontal and occipital border of Heschl's "complex" (the *sulcus temporalis transversus primus* and *secundus*), increases from approximately 1 cm occipito-medially to 3 cm fronto-laterally. This specific anatomy is reflected in the pattern of activity (Figs. 3B and 3C). The locations of the two HF areas near the occipito-medial border of HG (marked in blue; Fig. 3D) are directly comparable to the respective foci seen in subject FR1T. However, the two LF-activated fronto-lateral areas (marked in red) are clearly separated in the present case. When the bifurcation of Heschl's gyrus is considered, the activated areas are located at the respective frontal and occipital walls of Heschl's complex, and thus in the same relative position as in the above case.

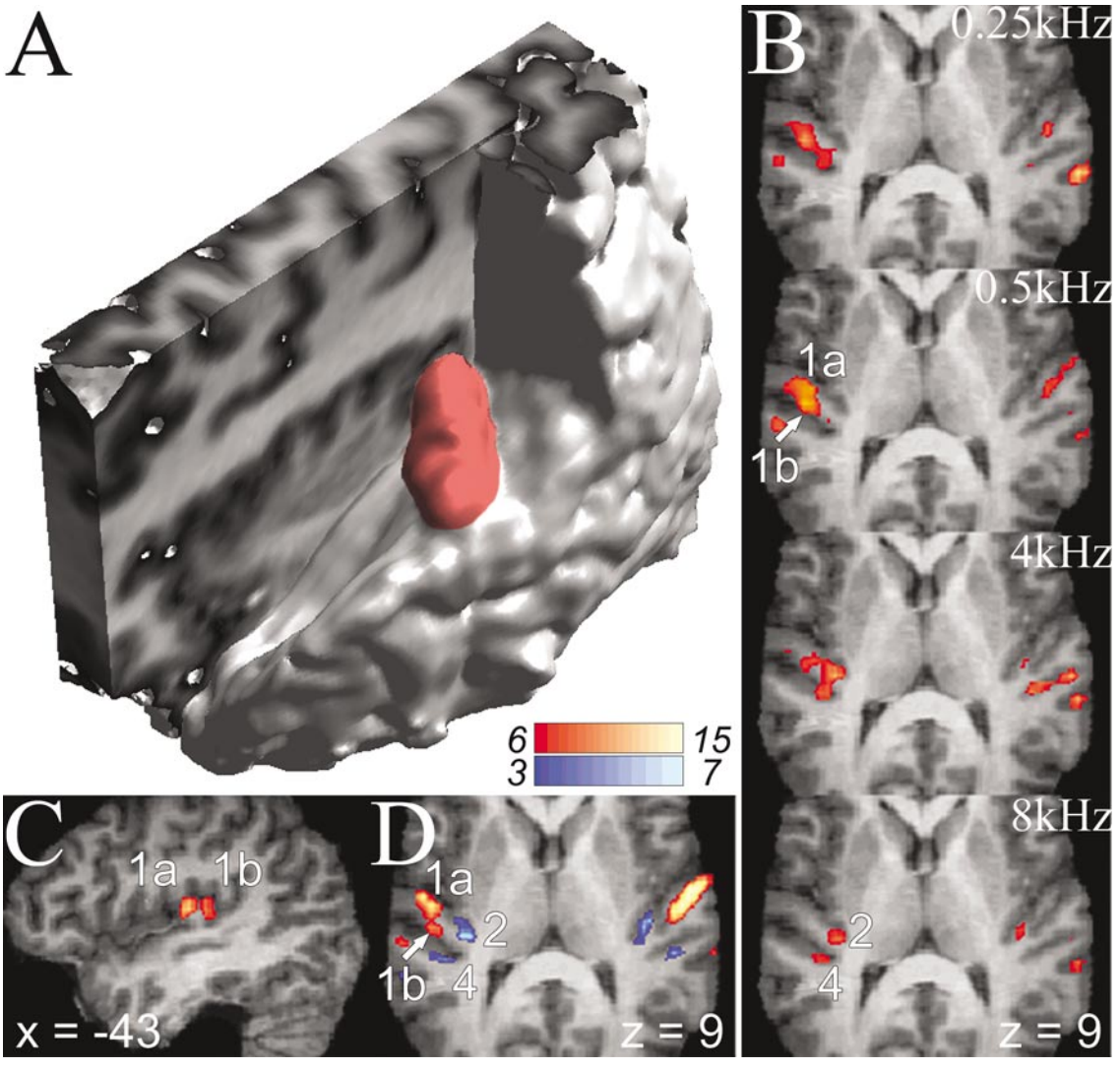


**FIG. 2.** Individual gyral pattern and distribution of activated areas in subject FR1T. (A) Three-dimensional reconstruction of the left temporal lobe with the STP surface exposed and Heschl's gyrus highlighted in red. (B) Activation pattern (SPM{Z}) for the four frequency conditions shown on an axial plane through the left Heschl's gyrus. The low-frequency stimulation caused lateral activation foci (1a and 1b, discernible in the upper two images, see text for further explanations) whereas high-frequency stimulation caused medial activation foci (2 and 4, lower two images). This difference is emphasized in (C) and (D) where low- and high-frequency conditions are contrasted. Foci with significant HF-dependent responses are shown in blue and LF foci in red. (D) The lateral LF activations coincide with the frontal and occipital walls of HG as seen on the parasagittal plane. Note that because of the small fronto-occipital extension of HG the lateral activation sites partly overlap.

The other 11 subjects showed the same correspondence between the individual anatomy of the superior temporal plane and the distribution of activated HF and LF areas.

*Frequency-Dependent Activity Patterns*

Since RFM stimuli have not been used in previous fMRI studies, the effects of increased bandwidth and of the more complex temporal signal structure on the cortical activation were tested. The actual differences in activation sites are shown for subject MA3T for which images were obtained by the use of both pure-tone and RFM stimuli (Fig. 4).

For this comparison, the pure-tone frequencies were set at the center frequencies of the respective RFM stimuli. As seen in Fig. 4, the RFM-induced activations were more prominent, and inevitably more spread out, than those induced by pure tones. Typically, the latter were located amidst the respective RFM activation sites. The major advantage of using RFM stimuli was that they gave prominence to the activation sites on lateral aspects of STP compared to pure tone stimulation.

Next, the typical pattern of frequency-specific activation sites will be described for subject HF1T, with special emphasis on those sites, which are consistently

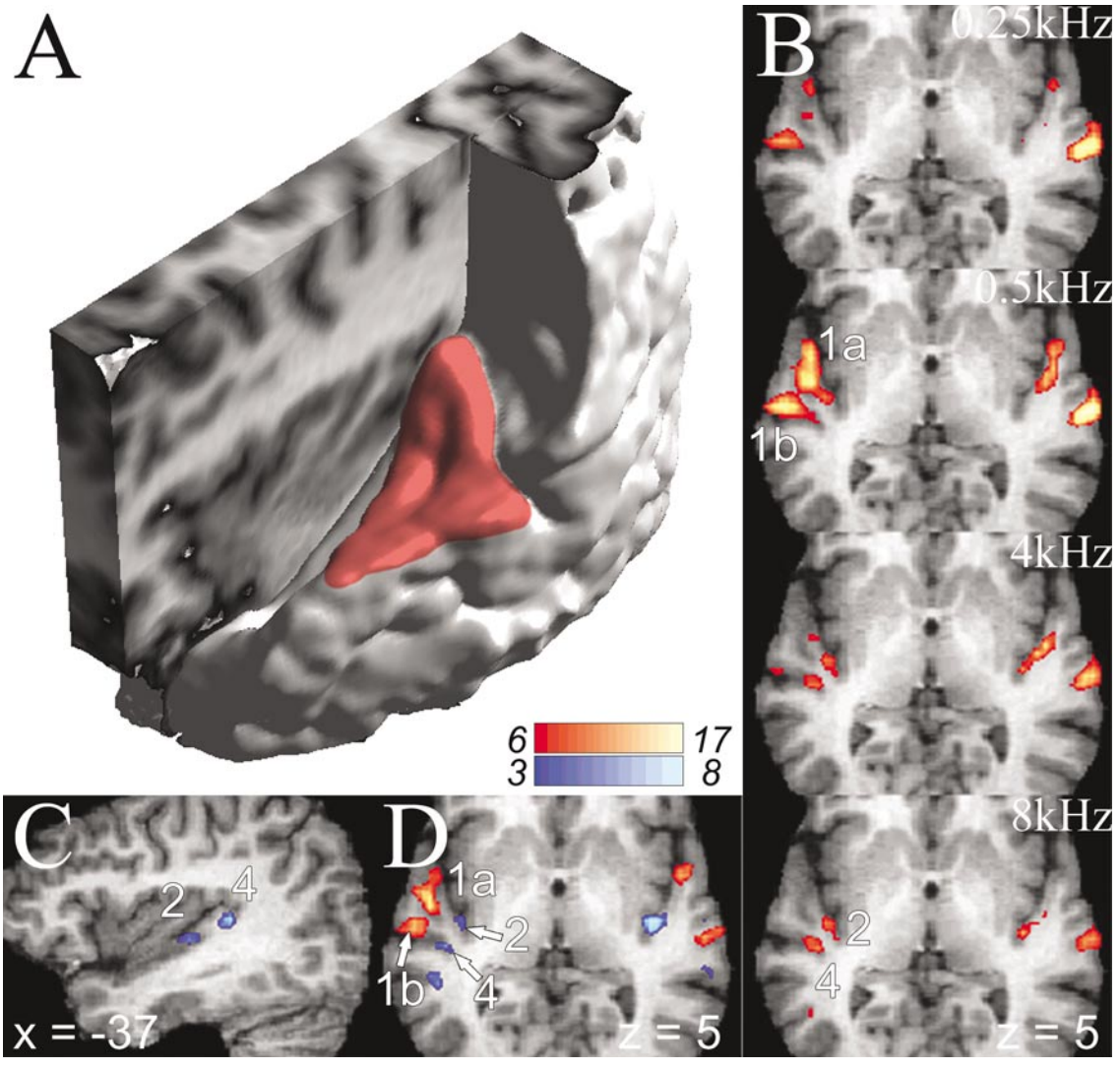


**FIG. 3.** Gyral pattern and distribution of activated areas in subject SJ2T. Details as in Fig 1. Note that the large fronto-occipital extension of HG due to its bifurcation causes the lateral activation sites (foci 1a and 1b, B and D) to be further apart than the respective foci in subject FR1T (Fig. 2). The parasagittal plane in (C) shows the medial HF foci (2 and 4) at the fronto- and occipito-medial walls of HG.

seen in all subjects (Fig. 5). Seven activation sites could be differentiated on the left STP, most of which showed a significant responsiveness during the four frequency conditions (Fig. 5A). The strength of activation, however, differed under either the high- (4.0 and 8.0 kHz) or the low-frequency conditions (0.25 and 0.5 kHz). Two foci located at the occipito-medial border of Heschl's gyrus (2 and 4, for an explanation of the nomenclature see below) showed a significantly stronger activation during the 4.0 and 8.0 kHz stimulation compared to the 0.25 and 0.5 kHz stimulation (Fig. 5B). The reverse accentuation of frequency-dependent response strength was seen in two fronto-lateral activation sites overlapping Heschl's gyrus (1a and 1b)

Three more foci were consistently found in all subjects. One with a prominent low-frequency activation was seen at the fronto-lateral transition of Heschl's gyrus to the STG (6). In the area of the planum temporale (PT) one high-frequency focus (3) was located occipital to HG and lateral to focus 4, approximately halfway on the medio-lateral PT extension (Fig. 5A, intermediate and superior planes). The frequency dependence of the last two foci (3 and 6) was less prominent than for foci 1a, 1b, 2, and 4, but still met the $P < 0.05$ significance criterion. The most occipital focus (8) was located where the STG bent toward the angular gyrus. In HF1T this focus did not show a significant frequency-dependent response, but had LF preference in the majority of the subjects. Two more activation sites are shown in Fig. 5A (∗ and ◆) which were not consistently found in the subjects. The first (∗), with a low-frequency preference, was located on the fronto-lateral PT and the second (◆), which did not show a significant frequency-dependent response extended over the occipital wall of HG in between focus 4 and focus 1b. In the intermediate and superior planes, foci

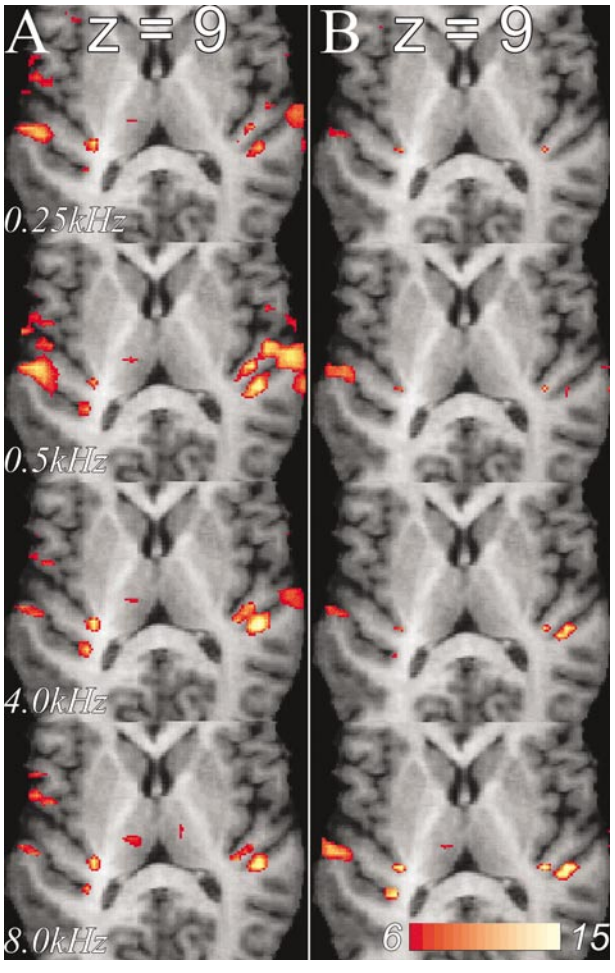


**FIG. 4.** Cortical activation in subject MA3T resulting from stimulation with (A) random-frequency modulation walks and (B) pure tones for four frequency conditions (0.25, 0.5, 4.0, and 8.0 kHz). The statistical parameter maps show $z$ values $>6.0$ ($P \ll 0.001$) overlaid on corresponding anatomical images. The pure-tone frequencies were set at the center frequencies of the respective RFM stimuli. Note that the RFM stimulation led to a more prominent activation particularly in the lateral STP.

∗ and ◆ merge with foci 1a and 1b, yielding a single large activation site (Fig. 5A).

*Grouped Data*

Averaging the centers of the individual specific activation sites in all 13 subjects using the Talairach coordinates as a reference gave evidence that the pattern of activation described above comprises distinct auditory processing domains on the STP (Fig. 6). For the identification of these frequency-responsive areas, the numbering scheme from Talavage and co-workers (2000) was adopted. Seven frequency-responsive foci could consistently be differentiated in the left hemisphere. Table 1 indicates the anatomical criteria for focus identification, the respective locations in Talairach coordinates, and the corresponding coordinates reported by Talavage and co-workers (2000).

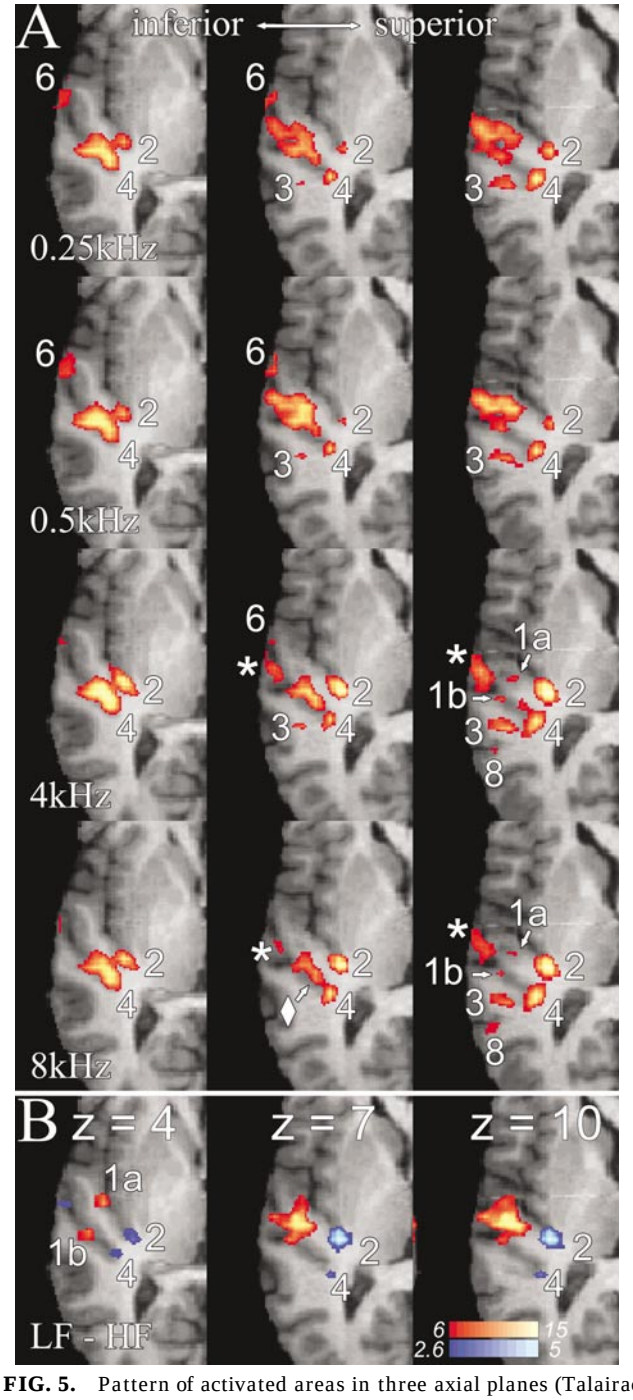


**FIG. 5.** Pattern of activated areas in three axial planes (Talairach $z = 4$, 7, and 10) for subject HF1T (SPM{Z}) overlaid on corresponding anatomical images. Each image is centered on Heschl's gyrus, which extends diagonally from occipito-medial to fronto-lateral. (A) The upper four rows show contrasts of the four frequency conditions vs baseline (0.25, 0.5, 4.0, 8.0 kHz). All voxels of the resulting $z$ maps with $z > 6.0$ ($P \ll 0.001$, uncorrected) are shown. Note that the large area of activation seen laterally in the intermediate and superior planes during low-frequency stimulation (0.25 and .5 kHz condition) separate into three distinct foci (1a, 1b, and *) with the RFMs shifted toward higher frequencies. (B) The bottom row (LF-HF) shows a contrast of the pooled low- vs pooled high-frequency conditions. The resulting $z$ maps depict areas with a significant difference ($P < 0.001$) in activation strength in the low-(marked in red) vs high-frequency conditions (marked in blue). The numbers indicate activation sites on HG and in its vicinity consistently found in the subjects.

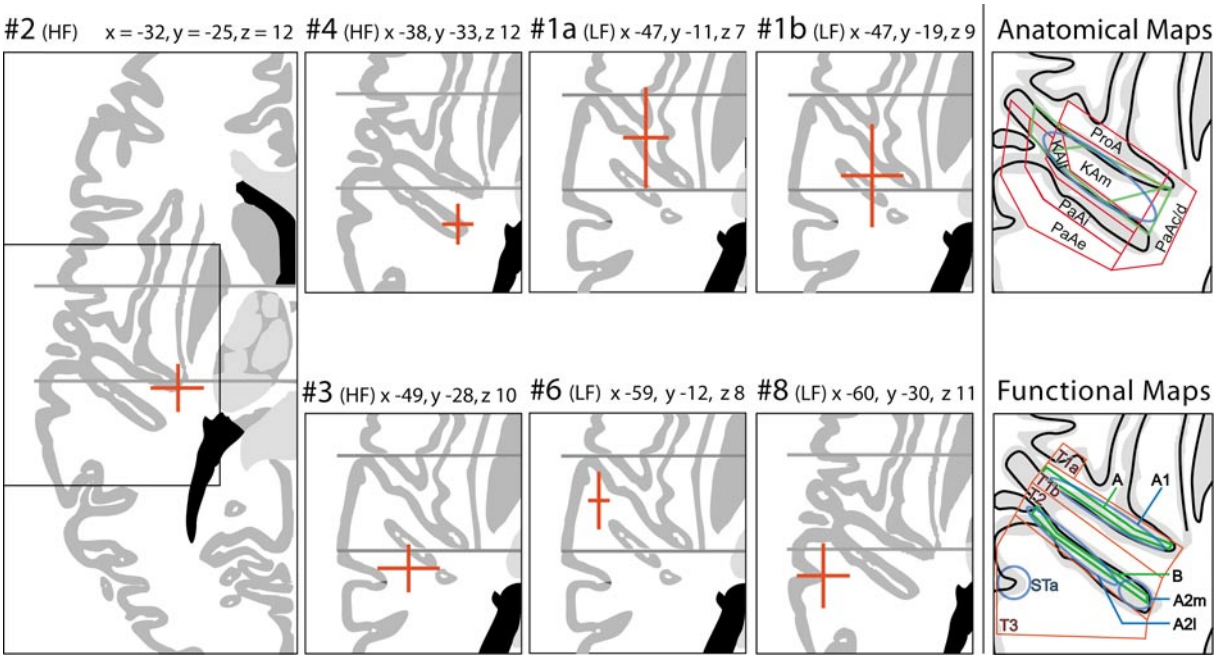


**FIG. 6.** The locations of seven frequency-dependent foci are shown on schematic outlines of the cortex based on the Talairach atlas (Talairach and Tournoux, 1988) [actual outlines are from the Talairach daemon (Lancaster *et al.*, 2000), an electronic version of the Talairach atlas; see http://ric.uthscsa.edu/projects/talairachdaemon.html]. The crossbars indicate the mean location and the 95% confidence area (corrected for DOF) of the respective foci. The header of each image gives the number of the depicted focus (adopted from Talavage *et al.*, 2000) followed by the frequency dependence (HF or LF) and the Talairach coordinates. Note the large fronto-occipital variance for foci 1a and 1b, which is due to the anatomical variability of HG across the subjects. The location of foci 2 and 4 showed the least variability. In order to facilitate comparison with results of other studies, the two right-most subfigures show fractions of relevant anatomical (Galaburda and Sanides, 1980; Rivier and Clarke, 1997; Morosan *et al.*, 2001) and functional maps (Scheich *et al.*, 1998; Hashimoto *et al.*, 2000; Di Salle *et al.*, 2001) overlaid on schematic drawings of HG and the surrounding cortex. The maps have been considerably simplified and the reader is advised to consult the original publications for further details of the parcellations. In the compilation of anatomical maps, only the cytoarchitectonical fields of Galaburda and Sanides (1980, outlined in red) are labeled (KAm, medial koniokortex; KAlt, lateral koniokortex; ProA, prokoniokortex; PaAi, internal parakonoikortex; PaAe, external parakoniokortex; PaAc/d, caudo-dorsal parakoniokortex). The large blue-encircled area covering most of HG in the same subfigure is AI of Rivier and Clarke (1997). The three adjoining areas outlined in green are fields Te 1.1, Te1.0, and Te1.2 (from medial to lateral HG) described by Morosan *et al.* (2001). In the compilation of functional maps shown in the lower right subfigure, the red outlines pertain to the functional fields T1a, T1b, T2, and T3 proposed by Scheich *et al.* (1998). The two green-encircled areas (A, B) were found to exhibit differential BOLD-response patterns (type a and type b decay pattern) during 1-kHz pure-tone stimulation by Di Salle *et al.* (2001). Finally, blue lines surround the areas described by Hashimoto *et al.* (2000, A1, A2m, and A21). The occipito-medial area A2m was differentially activated by a dichotic vs a diotic listening condition. (See Discussion for the proposed attribution of our activation foci to these maps.)

Foci 2 and 4 were the most stable activation sites across subjects in terms of location and frequency specificity (Fig. 6). They were found in all subjects and exhibited significantly greater activation strength during periods of high-frequency (4.0 and 8.0 kHz) compared to low-frequency stimulation (0.25 and 0.5 kHz). Foci 2 and 4 were also the most medially located activation sites overlapping with the frontal (focus 2) and the occipital wall (focus 4) of Heschl's gyrus at its medial border. Focus 3 was located on the PT occipital to HG and lateral to focus 4, approximately halfway on the medio-lateral PT extension. Focus 6 was located at the fronto-lateral transition of Heschl's gyrus to the STG. The latter two foci (3 and 6) were predominantly activated by low-frequency stimulation. Focus 8 was the most occipital activation site and occupied an area where the STG ascends toward the angular gyrus. This focus showed low-frequency dependence only in some subjects. What corresponds to Talavage's (2000) focus 1 could be further subdivided into two distinct low-frequency-responsive areas. One area, overlapping with HG fronto-laterally, was termed 1a and the other, located more occipital, 1b. The high standard errors in fronto-lateral direction for the mean location of foci 1a and 1b are an indication of the above-described anatomical variability of the lateral portions of HG (Fig. 6). No lateral shift of activation was observed when the stimulus frequencies were lowered from 0.5 to 0.25 kHz; neither did any other significant change in the location of the lateral activation site occur. Similarly, the 8 kHz stimulation did not induce activation more medial, or by other means different, than the 4 kHz activation.

The same pattern of frequency responsiveness was also seen on the right STP (not shown). Same as on the left side, the HF-activated foci were found occipito-

**TABLE 1**

Criteria for Identification of the Frequency-Responsive Foci with the Locations in Talairach Coordinates and the Mean Percentage Signal Change

| Focus | Criteria for designation | Talairach coordinates | *n* | Mean signal change (%) | Talairach coordinates Talavage *et al.* (2000) |
|---|---|---|---|---|---|
| 1a | LF focus on or near fronto-lateral wall of HG, not as lateral as focus 6, approx. as lateral as 3 | $x = -47.4 \pm 0.9$<br>$y = -11.1 \pm 1.9$<br>$z = 7.0 \pm 0.9$ | 12 | $0.71 \pm 0.1$ | Focus 1:<br>$x = -51.9 \pm 1.3$<br>$y = -16.3 \pm 1.9$<br>$z = 9.0 \pm 0.7$ |
| 1b | LF focus on or near occipito-lateral wall of HG, approx. as lateral as focus 1a | $x = -47.4 \pm 1.2$<br>$y = -19.0 \pm 2.0$<br>$z = 8.7 \pm 0.7$ | 13 | $0.81 \pm 0.1$ | |
| 2 | HF focus near fronto-medial extreme of HG, near junction with planum temporale | $x = -39.9 \pm 1.9$<br>$y = -25.2 \pm 1.8$<br>$z = 11.1 \pm 1.6$ | 13 | $-0.35 \pm 0.5$ | $x = -35.5 \pm 1.2$<br>$y = -18.5 \pm 1.8$<br>$z = 8.5 \pm 0.9$ |
| 4 | HF focus near occipito-medial extreme of HG, near the junction with the occipital parts of the insula | $x = -37.6 \pm 1.5$<br>$y = -32.8 \pm 1.7$<br>$z = 12.7 \pm 1.7$ | 13 | $-0.29 \pm 0.1$ | $x = -38.0 \pm 1.3$<br>$y = -34.0 \pm 2.3$<br>$z = 12.0 \pm 1.3$ |
| 3 | HF focus in or near medial part of the occipital Heschl sulcus, lateral and inferior to 4 & 2, medial to 8 | $x = -49.0 \pm 2.0$<br>$y = -28.2 \pm 1.8$<br>$z = 9.9 \pm 1.8$ | 13 | $-0.12 \pm .07$ | $x = -52.0 \pm 1.5$<br>$y = -25.5 \pm 1.7$<br>$z = 9.8 \pm 2.2$ |
| 6 | LF focus on or near fronto-lateral extreme of HG, as lateral as 8 and approximately as frontal as 1a | $x = -58.9 \pm 0.4$<br>$y = -12.4 \pm 1.0$<br>$z = 7.7 \pm 0.7$ | 12 | $0.43 \pm 0.1$ | $x = -59.6 \pm 1.5$<br>$y = -14.6 \pm 2.4$<br>$z = 10.6 \pm 1.3$ |
| 8 | (LF) focus on the STG, occipital to focus 6 and lateral to focus 3 | $x = -59.9 \pm 1.0$<br>$y = -29.9 \pm 1.3$<br>$z = 11.1 \pm 0.8$ | 12 | $0.1 \pm .06$ | $x = -59.6 \pm 1.2$<br>$y = -30.4 \pm 1.0$<br>$z = 10.7 \pm 1.3$ |

*Note.* Additionally, the coordinates reported by Talavage and co-workers (2000) are given for reference. The Talairach coordinates (mean ± SEM) are an average across foci locations in the left hemispheres of the subjects. Note that the percentage signal change is highest for activation sites 1a, 1b, 2, and 4 and decreases in the sites farer away from HG (secondary or tertiary auditory cortex).

medially and the LF foci fronto-laterally on Heschl's gyrus. Similarly, the anatomical intersubject variability increases from occipito-medial to fronto-lateral. Nevertheless, it was not possible to unequivocally distinguish as many separated activation sites on the right HG and in its vicinity. In nine subjects, the volumes of foci on the frontal border of Heschl's gyrus were connected with foci bordering the gyrus occipitally. The altered pattern on the right STP might relate to the fact that the right Heschl's gyrus is considerably narrower than its left counterpart is, so that the limit of imaging resolution prevents a more refined analysis.

### *Frequency Profiles along Heschl's Gyri*

The data presented indicate that acoustically evoked activation mainly coincides with the frontal and occipital walls of Heschl's gyrus. This suggests that variations of frequency-dependent activation might line up with these anatomical landmarks. In order to assess frequency-dependent activation along HG, we defined for each subject four tubulous regions of interest (two left and two right) exactly overlaying the individual frontal and occipital walls of HG (Fig. 7A). The strength of activation resulting from the stimulation in the four frequency bands was analyzed along each of these three-dimensional domains 21–42 mm in length. For subject ID1T, the frequency profiles are shown along the frontal (Fig. 7B, left) and occipital wall of HG (Fig. 7B, right). For all stimulus conditions, the response strength varied systematically along the spheres. Referring to the frontal wall of the left HG (Fig. 7B, left), the 4.0- and 8.0-kHz stimulation caused a significant activation near the medial border of Heschl's gyrus, while laterally under the same stimulus conditions there was a tendency for the activation to fall even below the resting level. The 0.25- and 0.5-kHz stimulation caused significant activation all along the frontal wall of HG with a broad maximum between 60 and 90% of its longitudinal extension. For the occipital HG wall (Fig. 7B, right), the variation of activation strength resulting from LF stimulation showed a similar gradient with the maximum activation in the lateral half of HG. The activation caused by HF stimulation was maximal at the medial HG border, where it exceeded the LF-induced activation and decreased toward the lateral HG. The same frequency gradients were also observed for the frontal and occipital walls of HG on the right side (not shown).

Averaging the frequency profiles for all 13 subjects for the left and the right STP (Fig. 8) revealed frequency-dependent response patterns matching with those shown for subject ID1T (Fig. 7). Medial portions of HG responded more vigorously to high-frequency and lateral portions predominantly to low-frequency stimula-

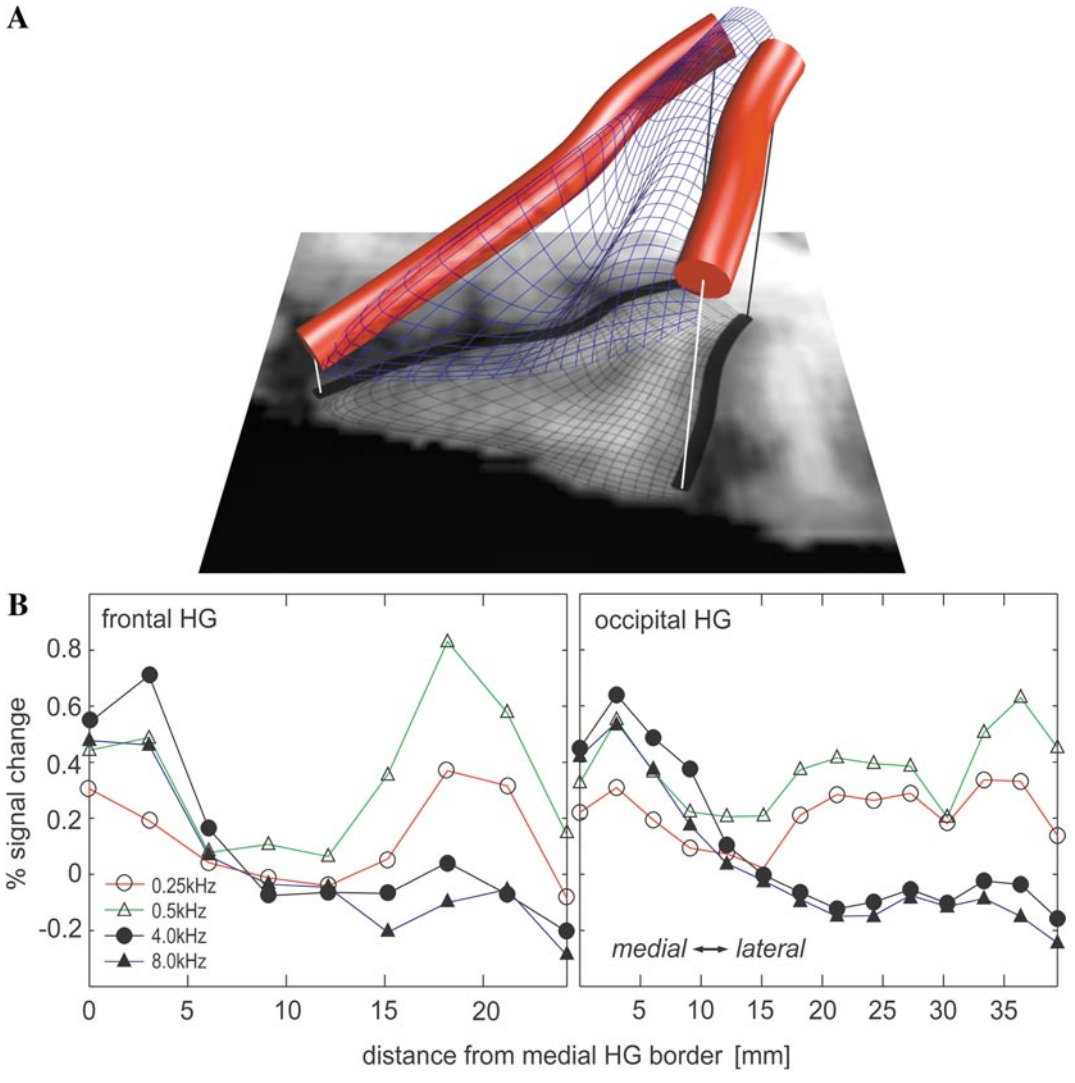


**FIG. 7.** Tubular regions of interest (ROI) used to extract individual frequency profiles along Heschl's gyri. (A) Two tubular ROIs were manually aligned with the frontal and occipital walls of Heschl's gyrus. (B) The relative activation strength of voxels in the four frequency conditions analyzed from medial to lateral along the regions indicated in (A) at the frontal and occipital wall of HG.

tion. Difference in activation strength were highly significant in medial and lateral HG portions, but not in a transition area between both.

### *Variation of the Frequency Selectivity along Heschl's Gyrus*

The frequency profiles showed nonsymmetrical gradients for high- and low-frequency responses (Fig. 9). The fronto-medial and occipito-medial portions of HG were activated by both low and high frequencies, but with the HF significantly surpassing the LF activation. In contrary, the fronto-lateral and occipito-lateral portions of Heschl's gyrus were almost exclusively activated by low-frequency stimulation. High frequencies did not cause significant activations. The level of frequency selectivity can be assessed by quantifying the difference in activation strength caused by high- and low-frequency stimulation (Fig. 9). In all four HG domains, this analysis showed a similar increase of the frequency selectivity from medial to lateral portions of HG. This analysis also revealed that the frequency profiles along HG on the right and the left STP were almost identical.

## DISCUSSION

The present results provide evidence for multiple frequency-dependent activation sites on the STP. The anatomical intersubject variability of Heschl's gyrus was recognized as the major source of functional intersubject variability. By examining the variation of frequency-dependent activity along individual Heschl's gyri—the main landmarks of the auditory cortex—we found that (a) the response strength resulting from high- and low-frequency stimulation varies systematically in opposite directions along HG and (b) the degree

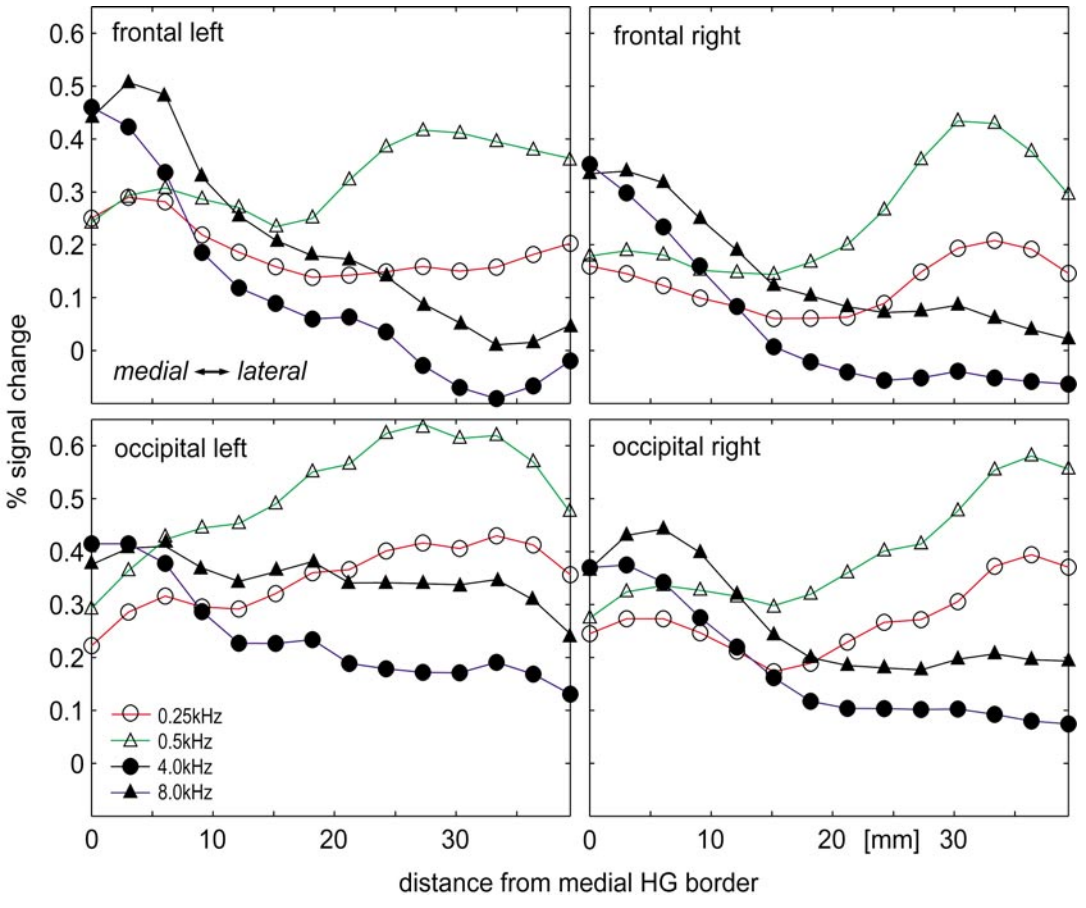


**FIG. 8.** Averaged frequency profiles for the frontal and occipital walls of the left and right Heschl's gyri (frequencies indicated in the graph). The strength of activation caused by high-frequency stimulation decreases from medial to lateral in the four domains analyzed. Low-frequency stimulation caused maximum activation in the lateral third of the medio-lateral HG extension. Note the differences between the frontal and the occipital frequency profiles as well as between the medial and the lateral HG portions.

of frequency selectivity increases from medial to lateral.

Because of technical limitations and the need for averaging the data from many subjects, early imaging studies identified only a medial high- and a lateral low-frequency activation site on STP (Lauter *et al.*, 1985; Wessinger *et al.*, 1997). Still, the results were considered as an indication of a tonotopic organization of the auditory cortex. This finding was inconsistent with electrophysiological studies in nonhuman primates, in which multiple tonotopic maps within the primary auditory cortex were reported (Merzenich and Brugge, 1973; Imig *et al.*, 1977; Morel and Kaas, 1992; Morel *et al.*, 1993). It seems likely that these imaging studies only detected the most prominent activation sites with a high degree of frequency selectivity, namely 1a and 1b jointly as one lateral LF activation site, and 2 and 4 as a single medial HF activation site.

More recent imaging studies were devoted to also reveal a more complex tonotopic parcellation in the human auditory cortex. Undeniably, these studies succeeded in differentiating multiple activation sites on STP, but the attribution of those sites to cytoarchitectonically defined areas still requires more in-depth analyses. There are a number of basic factors to be considered when one tries to line up imaging and cytoarchitectonical data. First, it is not entirely clear how many activation foci found in a functional image correspond to a single cytoarchitectonically defined field. The argument is as follows: (1) Combined cytoarchitectonical and electrophysiological studies in nonhuman primates point to a clear correspondence between anatomically and physiologically defined fields to an extent that cellular response properties can be used as markers for cytoarchitectonical field borders (Tian *et al.*, 2001). (2) Electrophysiological studies disclose clear tonotopic organization in the primary auditory cortex but only in one of the secondary (Rauschecker *et al.*, 1995) and none of the tertiary areas. The primary (core) area embodies two (rhesus monkey, Merzenich and Brugge, 1973; Imig *et al.*, 1977; Morel *et al.*, 1993) or three (owl monkey, Morel and Kaas, 1992; Hackett *et al.*, 1998; Kaas and Hackett, 1998, 2000) more or less complete tonotopic maps. (3) With the exception of the field CM (Rauschecker *et al.*, 1995), the secondary (auditory belt) and tertiary (auditory parabelt) fields did

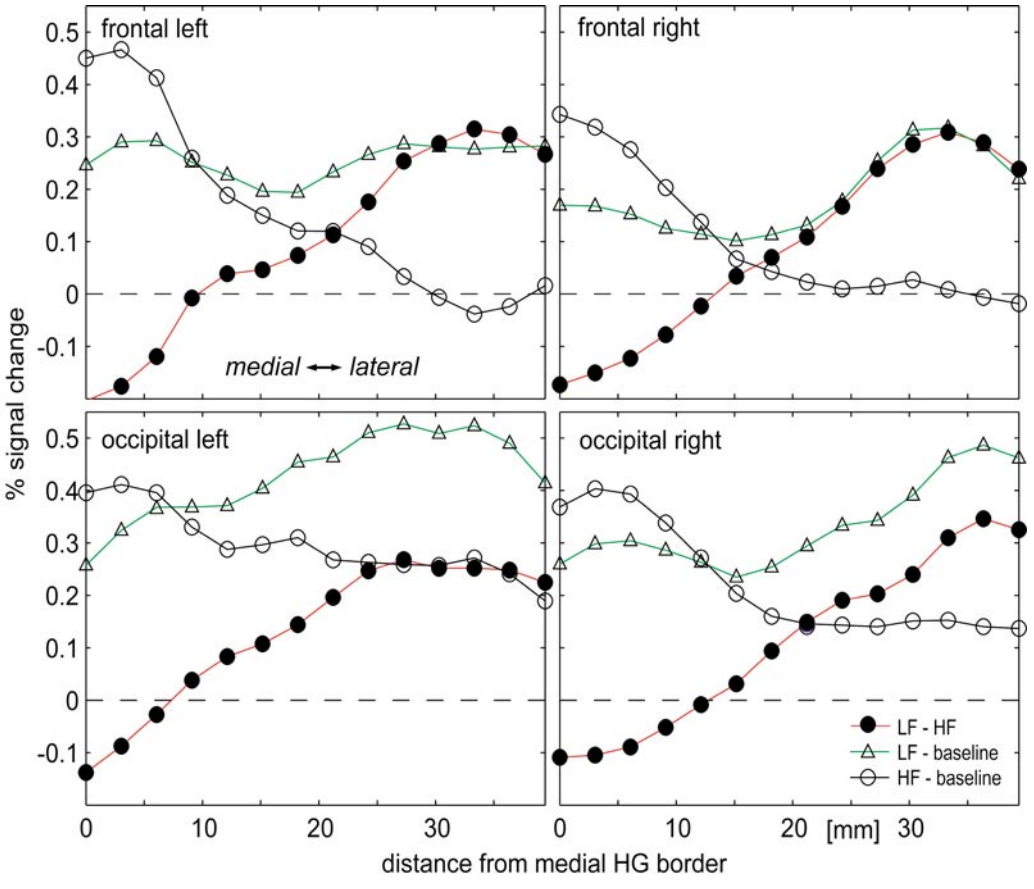


**FIG. 9.** Average frequency selectivity for the frontal and occipital walls of the left and right Heschl's gyri. The frequency selectivity was quantified by the mean percentage signal change between the LF and HF stimulus conditions (LF − HF). Note that the frequency selectivity increases from medial to lateral in all four domains analyzed. The lateral LF-responsive areas are highly selective for low frequencies (LF − baseline), whereas the medial HF areas are activated by both low and high frequencies with the HF activation strength surpassing the LF activation strength (HF − baseline and LF − baseline).

not exhibit a distinctive tonotopy. Consequently, frequency-dependent activation foci should be predominantly found in the area of the primary auditory cortex, i.e., the medial two thirds of HG, while, toward higher auditory areas, like belt and parabelt, the frequency selectivity should decrease. The attribution of activation foci to cytoarchitectonical fields is often based on the euclidean distance in Talairach space between the centers of mass of such foci and the centers of the respective cytoarchitectonical fields. This mostly results in a one-to-one correspondence of foci to fields. While this procedure undoubtedly yields an objective parameter (the distance) for establishing such a correspondence, it completely ignores the underlying physiology and seems inappropriate to arrive at conclusions regarding the tonotopic organization. One frequency-dependent activation focus in a cytoarchitectonical field (regardless whether selective to high or low frequencies) cannot be considered as indication of a tonotopic organization, since such an indication would presuppose at least two activation foci of opposing frequency selectivity in a single cytoarchitectonical field. While we currently also propose a correspondence between the seven activation foci and parcellations based on cytoarchitectonical criteria, we still arrive at different conclusions regarding tonotopic organization.

Another critical issue inherent in fMRI is the effect draining veins have on the localization of BOLD-response activation foci. These veins can be small and hard to detect. The location of activation foci might depend on the individual vein pattern rather than on the individual functional parcellation of the cortex. Still, we would argue that the location of the present activation foci, especially of the foci at the frontal and occipital walls of HG, is an indication of functional parcellation rather than a reflection of the course of draining veins. The argument rests on the finding of differences of the BOLD-response properties of frontal and occipital areas on HG found in the present study and in other recent studies detailed below. The assumption that foci on the frontal and occipital wall of HG are merely a single activated area dispersed by the effects of veins running along either wall of HG implies that these areas should be coactivated under all experimental conditions. This is not the case, as shown by Hashimoto *et al.* (2000). Furthermore, the location of

veins and activation foci on STG was found to be uncorrelated by Di Salle *et al.* (2001). Nonetheless, it can be that the exact localization of fMRI foci is affected by the course of veins, e.g., veins that run in the sulcal basins might shift the foci away from the crown of HG toward the depth of the limiting sulci. While this would weaken the comparability of fMRI data with electrophysiological data, it will not impede the comparability of different fMRI studies.

The cytoarchitectonical maps of the auditory cortex that we will refer to are those reported by Galaburda and Sanides (1980), Rivier and Clarke (1997), and Morosan *et al.* (2001). Our attempt was complicated by the fact that in these three studies the parcellation of Heschl's gyrus differs. Originally, Galaburda and Sanides (1980) differentiated two koniocortical fields: KAm, occupying the fronto-medial wall, and the crown of HG and KAlt, occupying the lateral crown and stretching into the occipitally bordering sulcus. More recently, Rivier and Clarke (1997) identified only a single large field, termed A1, covering most of HG. Morosan *et al.* (2001) [whose parcellation refines the primary auditory cortex (TC) in the classical map from von Economo and Koskinas (1925)] emphasized medio-lateral cytoarchitectonical differences along HG by distinguishing three adjoining areas, Tel.1, Tel.0, and Tel.2.

Of the currently identified activation sites, focus 1a (Fig. 6) is the most likely candidate for a response from the primary auditory cortex, as it lies directly on the fronto-lateral surface of HG in all subjects. This activation site corresponds to parts of KAm, A1 and Tel.0 (here and in the remainder of the paragraph the respective abbreviations point to the three studies of Galaburda and Sanides, Rivier and Clarke, and Morosan *et al.*). Focus 1b, which lies in the sulcus bordering HG occipitally, could be attributed to KAlt (primary auditory cortex) or to PaAi (secondary auditory cortex) of Galaburda and Sanides. With reference to the parcellation of Rivier and Clarke, 1b can also equally well be attributed to the primary or the secondary auditory cortex, the fields A1 or LA, respectively. Focus 2 is located near the fronto-medial border of HG, where, according to Galaburda and Sanides, three cytoarchitectonical fields adjoin, impeding an unequivocal attribution of this focus to one of them. KAm extends medio-laterally on HG and is bordered frontally alongside the first sulcus of Heschl by ProA, which covers a portion of the planum frontale. Both fields stretch up to the posterior caudo-dorsal paraconiocortex (PaAc/d) at the fronto-medial border of HG. Rivier and Clarke did not include this area in their cytoarchitectonical analysis. Their fields A1 on HG as well as MA (which resembles ProA of Galaburda and Sanides) do not cover the most fronto-medial extends of HG and the frontally bordering sulcus. Still, A1 is the best choice for attributing focus 2. Referring to the map of Morosan and co-workers focus 2 corresponds to the field Tel.1 that covers the entire medial portion of HG.

The same field also comprises focus 4, located just occipitally from 2 near the occipito-medial border of HG. Focus 4 is difficult to match with the map of Galaburda and Sanides as four cytoarchitectonical fields (KAm, KAlt, PaAi, and PaAc/d) meet at its location. In the map of Rivier and Clarke, the field PA occupies the occipito-medial portion of HG and parts of the medial planum temporale, a location that is in good correspondence with the location of focus 4.

The location of focus 3 on the planum temporale is consistent with field PaAi of Galaburda and Sanides, which stretches occipitally from HG along frontal aspects of the planum temporale. In the map of Rivier and Clarke, this location is occupied by the field LA. Focus 6 and 8 are located near the rim between STP and the superior temporal gyrus (STG), a region termed auditory parabelt which is thought to embody the tertiary auditory cortex. With reference to Galaburda and Sanides' nomenclature, foci 6 and 8 lie in the region of the internal and external parakoniocortex (PaAi, PaAe). With regard to the map of Rivier and Clarke only focus 8 would correspond to the superior temporal area (STA), whereas focus 6 lies just frontal of it at the fronto-lateral extreme of HG. The latter location does not correspond to one particular field in their map.

The aforementioned four foci, 1a, 1b, 2, and 4 would be the best choice if one considers a tonotopic organization of the auditory cortex. However, the apparent ambiguity of the anatomical attribution of the four foci makes it unlikely that all four correspond to the primary auditory cortex. Additionally, recent experimental evidence suggests that the activation near the occipital border of HG seen in imaging studies (our 1b and 4) is a response from secondary auditory cortex (see below). The remaining foci 3, 6, and 8 cluster around HG and might correspond to secondary and tertiary auditory areas.

### *Comparison with Physiological Data*

At least as important as the anatomical attribution is the correspondence of activation foci between recent imaging studies. The activation sites found in the present study show a good correspondence to activation patterns reported by Hashimoto *et al.* (2000), Talavage *et al.* (2000), Scheich *et al.* (1998), and Di Salle *et al.* (2001). In these studies, characteristic "stripe-like" clusters of auditory activation were found with maxima arranged alongside the frontal and occipital walls of HG. Additional activation sites were reported on PT. Taken together, the studies suggest a physiological distinction between the frontal and the occipital wall of HG, whereby the frontal wall corresponds to the primary and the occipital wall to the secondary auditory cortex (Scheich *et al.*, 1998; Hashimoto *et al.*, 2000;

Di Salle *et al.*, 2001). The latter can be further subdivided into a medial and lateral portion by their specific response properties (Hashimoto *et al.*, 2000). Our activation sites can be associated with the functional fields proposed in these studies on the basis of anatomical ties. The activation sites on the frontal HG (1a and 2) lie in the area T1b of Scheich *et al.* (1998), while the occipital (1b and 4) lie in T2. Area T3, as described in the same paper, covers most of PT and includes the anatomical locus of our foci 3 and 8. Hashimoto (2000) described (among other results) three activated areas on STP (A1, A2m, and A2l). The activation site A1 extends along the frontal wall of HG, covering an area comparable to our foci 1a and 2. Their activation site A2, stretching along the occipital wall of HG, was further divided into a medial (A2m) and a lateral portion (A2l). The locations of these two sites correspond with our foci 1b and 4. Di Salle and co-workers (2001) described distinct activation clusters along the frontal and occipital walls of HG, which differed in the time course of the hemodynamic response. The frontal activation covers the anatomical locations of our foci 1a and 2, whereas the occipital one covers foci 1a and 4.

In the context of previous results, the present findings support the notion of physiological differences between medial/lateral and frontal/occipital portions of HG. On the frontal wall the HF activation decreases laterally to zero, while on the occipital wall it does not. Furthermore is the frequency selectivity in the lateral low-frequency parts of the frontal and occipital HG walls significantly greater than in the medial parts. This concept is consistent with differences in BOLD-response properties (between frontal and occipital HG; Di Salle *et al.*, 2001), sensitivity to task and stimulus differences (occipito-medial and occipito-lateral HG; Hashimoto *et al.*, 2000), and location of activation foci (Scheich *et al.*, 1998; Talavage *et al.*, 2000; Hashimoto *et al.*, 2000; Di Salle *et al.*, 2001). These physiological differences lessen the likelihood of a combination of different pairs of activation foci as endpoints of tonotopic representations. An alternative interpretation is that the activation sites correspond to different cortical fields, the topological organization of which cannot be resolved with the spatial resolution of several millimeters. In this notion, the detected frequency selectivity of different cortical areas arises from an excess of neurons engaged in the processing of different acoustic features, which are associated with different frequency bands.

### *Frequency Profiles*

The frequency profiles show the variation of activation strength along individual Heschl's gyri for the four frequency conditions. This analysis is based on the assumption that HG can be used as marker for the primary and secondary auditory cortex.

Heschl's gyrus was taken as a landmark for the primary auditory cortex since Flechsig's original article in 1908. Recently, at least two cytoarchitectonical studies have questioned the reliability of the relationship between the macroanatomical landmark, HG, and the exact course of microanatomical area borders (Hackett *et al.*, 2001; Morosan *et al.*, 2001). Both studies state that it is not possible to *precisely* localize the borders of the primary auditory cortex. Hackett and co-workers (2001) report that, in the case of a duplication of HG, the auditory core field may occupy variable portions of both gyri, spanning the intermediate sulcus. In the case of one HG, the core occupied most of its surface and was constrained by its sulcal boundaries (Hackett *et al.*, 2001). Morosan and co-workers (2001) state that a comparison of the Talairach coordinates of the transverse sulci and those of the borders of primary auditory cortex show significant discrepancies between both markers. We agree that this is true for the submillimeter and millimeter scale. Nevertheless, we think that given the in-plane resolution of $3 \times 3$ mm of the present and many other fMRI studies, and taken into account that MRI permits no direct access to the microanatomy of individual subjects, the HG still provides the best estimate for the location of primary auditory cortex.

The medial portions of the frontal and occipital walls of HG responded predominantly to high frequencies, while lateral portions were more active during low-frequency stimulation. Assuming the high- and low-frequency activation sites as indicators of tonotopy, one would expect a systematic decrease of LF-induced activation toward medial portions of HG and a corresponding increase in HF-induced activation. However, such systematic gradients were not observed. Medial portions of HG were more balanced in their responses to LF and HF stimulation, with the HF slightly surpassing the LF activation. On the contrary, lateral portions of HG almost exclusively showed LF activation. This difference in frequency selectivity further adds to the notion of a functional medio-lateral distinction of HG and renders it difficult to combine medial and lateral activation sites as endpoints of a single tonotopic representation. In the alternative interpretation, that the different activation sites correspond to different cortical fields, the detected frequency selectivity stems from an excess of neurons tuned to high or low frequencies. The differences in overall frequency tuning in different neuronal populations could arise from their engagement in the processing of different acoustic features, which are associated with different frequency bands. Medio-lateral differences in feature processing on HG have been proposed for humans and nonhuman primates. A concept adapted from research in the visual domain is the distinction of auditory processing streams for object recognition and spatial information (Tian *et al.*, 2001; Rauschecker and Tian, 2000; Romanski *et al.*, 1999). Most of the spectral cues

important for spatial localization of sound sources lie in higher frequency bands, whereas human speech is confined to lower frequencies. Another emerging concept is that spectral and temporal features are preferentially processed at the medial and lateral HG, respectively (Hall *et al.*, 2002; Griffiths *et al.*, 2001). Again, if most of the relevant spectral and temporal cues are assumed to lie in different frequency bands this would lead to a different preferential frequency tuning of medial and lateral auditory areas. The frequency selectivity, defined as the percentage signal change between HF and LF stimulation, was highest at the lateral activation sites 1a and 1b, followed by 2 and 4 at the medial border of HG. The remainder of activation sites (3, 6, 8) showed a lesser degree of frequency selectivity, just reaching statistical significance. This low degree of frequency selectivity of secondary and tertiary areas is more likely to correspond to functional specialization than to tonotopic gradients (see above).

### *Anatomical Variation*

The anatomical variability of Heschl's gyrus found in the subjects is in good agreement with data from recent morphological studies. Penhune and co-workers (1996) reported an incidence of 20% for duplications of HG in a quantitative MRI study on normal subjects. Leonard and co-workers (1998), using a more refined analysis, concluded that the incidence of HG duplications increases with the distance from the sagittal plane. The incidence of what the authors called "common stem duplications" (i.e., where the gyrus bifurcates at some point between the medial and lateral end) increased up to 40% on the left and 50% on the right STP. Complete duplications reaching up to the medial base of HG were only found in 20% of the subjects. In our subjects, 38% (5/13) of the left and 46% (6/13) of the right Heschl's gyri bifurcated and no complete duplications were detected. This variable duplication pattern is most prominent at lateral aspects of HG and explains the laterally increased variance of the distance between frontal and occipital walls of HG (see Fig. 1B).

The finding that the HG anatomy constitutes a major source of interindividual functional variability has implications for future group studies on the auditory cortex. Two procedures are commonly used to normalize groups of brain volumes: transformation into Talairach-Fox space and brain warping. Neither of these procedures can adequately deal with the high anatomical variability of STP. If several functional volumes are subjected to one or to both transformations in order to create an average activation map, the more subtle activations tend to cancel out. Thus, if possible, the distribution of activation sites should be studied in individual subjects. If activation sites are to be compared across subjects, regions of interest can be defined, aligned with individual anatomical landmarks. Another possibility is to select subjects according to their HG bifurcation pattern, since warping algorithms can usually handle a consistent number of gyri on STP.

The apparent interindividual differences in length and width of Heschl's gyri and the associated differences in the extension of cortical areas impose the question of possible functional significance. We are currently engaged in a study, which aims at the correlation of individual extensions of STP regions with differences in basic auditory discrimination performance.

In sum, (i) the combination of physiologically plausible RFM stimuli differing in spectral content, (ii) an analysis referring to the individual gyral pattern, and (iii) a careful comparison of the activation sites with cytoarchitectonical and imaging studies sheds new light on the results of earlier attempts to reveal the tonotopic organization of auditory areas of STP. A hypothesis of how to interpret the activation pattern on STP, which we think fits the known cytoarchitectonical and physiological properties of the involved cortical areas better, was suggested.

## ACKNOWLEDGMENTS

This work has been founded by the Deutsche Forschungsgemeinschaft CR 43 / 13-1. M.S. is supported by a grant from the German Merrit Foundation.

## REFERENCES

Bilecen, D., Scheffler, K., Schmid, N., Tschopp, K., and Seelig, J. 1998. Tonotopic organization of the human auditory cortex as detected by BOLD-FMRI. *Hearing Res.* **126:** 19–27.

Di Salle, F., Formisano, E., Seifritz, E., Linden, D. E., Scheffler, K., Saulino, C., Tedeschi, G., Zanella, F. E., Pepino, A., Goebel, R., and Marciano, E. 2001. Functional fields in human auditory cortex revealed by time-resolved fMRI without interference of EPI noise. *NeuroImage* **13:** 328–338.

Edmister, W. B., Talavage, T. M., Ledden, P. J., and Weisskoff, R. M. 1999. Improved auditory cortex imaging using clustered volume acquisitions. *Hum. Brain Mapp.* **7:** 89–97.

Fitzpatrick, K. A., and Imig, T. J. 1980. Auditory cortico-cortical connections in the owl monkey. *J. Comp. Neurol.* **192:** 589–610.

Flechsig, P. 1920. Bemerkungen über die Hörsphäre des menschlichen Gehirns. *Neurol. Cbl* **27:** 2–7, 50–57.

Friston, K. J., Frith, C. D., Turner, R., and Frackowiak, R. S. 1995a. Characterizing evoked hemodynamics with fMRI. *NeuroImage* **2:** 157–165.

Friston, K. J., Holmes, A. P., Poline, J. B., Grasby, P. J., Williams, S. C., Frackowiak, R. S., and Turner, R. 1995b. Analysis of fMRI time-series revisited. [see comments]. *NeuroImage* **2:** 45–53.

Galaburda, A., and Sanides, F. 1980. Cytoarchitectonic organization of the human auditory cortex. *J. Comp. Neurol.* **190:** 597–610.

Galaburda, A. M., and Pandya, D. N. 1983. The intrinsic architectonic and connectional organization of the superior temporal region of the rhesus monkey. *J. Comp. Neurol.* **221:** 169–184.

Grady, C. L., Van Meter, J. W., Maisog, J. M., Pietrini, P., Krasuski, J., and Rauschecker, J. P. 1997. Attention-related modulation of

activity in primary and secondary auditory cortex. *NeuroReport* **8:** 2511–2516.

Griffiths, T. D., Uppenkamp, S., Johnsrude, I., Josephs, O., and Patterson, R. D. 2001. Encoding of the temporal regularity of sound in the human brainstem. *Nature Neurosci.* **4:** 633–637.

Hackett, T. A., Stepniewska, I., and Kaas, J. H. 1998. Subdivisions of auditory cortex and ipsilateral cortical connections of the parabelt auditory cortex in macaque monkeys. *J. Comp. Neurol.* **394:** 475–495.

Hall, D. A., Johnsrude, I. S., Haggard, M. P., Palmer, A. R., Akeroyd, M. A., and Summerfield, A. Q. 2002. Spectral and temporal processing in human auditory cortex. *Cereb. Cortex* **12:** 140–149.

Hall, D. A., Haggard, M. P., Akeroyd, M. A., Palmer, A. R., Summerfield, A. Q., Elliott, M. R., Gurney, E. M., and Bowtell, R. W. 1999. "Sparse" temporal sampling in auditory fMRI. *Hum. Brain Mapp.* **7:** 213–223.

Hashimoto, R., Homae, F., Nakajima, K., Miyashita, Y., and Sakai, K. L. 2000. Functional differentiation in the human auditory and language areas revealed by a dichotic listening task. *NeuroImage* **12:** 147–158.

Howard, M. A., 3rd, Volkov, I. O., Abbas, P. J., Damasio, H., Ollendieck, M. C., and Granner, M. A. 1996. A chronic microelectrode investigation of the tonotopic organization of human auditory cortex. *Brain Res.* **724:** 260–264.

Imig, T. J., Ruggero, M. A., Kitzes, L. M., Javel, E., and Brugge, J. F. 1977. Organization of auditory cortex in the owl monkey (Aotus trivirgatus). *J. Comp. Neurol.* **171:** 111–128.

Kaas, J. H., and Hackett, T. A. 1998. Subdivisions of auditory cortex and levels of processing in primates. *Audiol. Neuro-Otol.* **3:** 73–85.

Kaas, J. H., and Hackett, T. A. 2000. Subdivisions of auditory cortex and processing streams in primates. *Proc. Natl. Acad. Sci. USA* **97:** 11793–11799.

Lancaster, J. L., Woldorff, M. G., Parsons, L. M., Liotti, M., Freitas, C. S., Rainey, L., Kochunov, P. V., Nickerson, D., Mikiten, S. A., and Fox, P. T. 2000. Automated Talairach atlas labels for functional brain mapping. *Hum. Brain Mapp.* **10:** 120–131.

Lauter, J. L., Herscovitch, P., Formby, C., and Raichle, M. E. 1985. Tonotopic organization in human auditory cortex revealed by positron emission tomography. *Hearing Res.* **20:** 199–205.

Leonard, C. M., Puranik, C., Kuldau, J. M., and Lombardino, L. J. 1998. Normal variation in the frequency and location of human auditory cortex landmarks. Heschl's gyrus: Where is it? *Cereb. Cortex* **8:** 397–406.

Lockwood, A. H., Salvi, R. J., Coad, M. L., Arnold, S. A., Wack, D. S., Murphy, B. W., and Burkard, R. F. 1999. The functional anatomy of the normal human auditory system: Responses to 0.5 and 4.0 kHz tones at varied intensities. *Cereb. Cortex* **9:** 65–76.

Lohmann, G., Mueller, K., Bosch, V., Mentzel, H., Hessler, S., Chen, L., and von Cramon, D. Y. 2001. Lipsia—A new software system for the evaluation of functional magnetic resonance images of the human brain. *Comput. Med. Imaging Graphics* **25:** 449–457 (see also: http://www.cns.mpg.de/lipsia).

Merzenich, M. M., and Brugge, J. F. 1973. Representation of the cochlear partition of the superior temporal plane of the macaque monkey. *Brain Res.* **50:** 275–296.

Mesulam, M. M., and Pandya, D. N. 1973. The projections of the medial geniculate complex within the sylvian fissure of the rhesus monkey. *Brain Res.* **60:** 315–333.

Morel, A., Garraghty, P. E., and Kaas, J. H. 1993. Tonotopic organization, architectonic fields, and connections of auditory cortex in macaque monkeys. *Journal of Comp. Neurol.* **335:** 437–459.

Morel, A., and Kaas, J. H. 1992. Subdivisions and connections of auditory cortex in owl monkeys. *J. Comp. Neurol.* **318:** 27–63.

Morosan, P., Rademacher, J., Schleicher, A., Amunts, K., Schormann, T., and Zilles, K. 2001. Human primary auditory cortex: cytoarchitectonic subdivisions and mapping into a spatial reference system. *NeuroImage* **13:** 684–701.

Norris, D. G. 2000. Reduced power multi-slice MDEFT imaging. *J. Magn. Reson. Imaging* **11:** 445–451.

Ojemann, G. A. 1983. Brain organization for language from the perspective of electrical stimulation mapping. *Behav. Brain Sci.* 189–230.

Oldfield, R. C. 1971. The assessment and analysis of handedness: The Edinburgh inventory. *Neuropsychologia* **9:** 97–113.

Pandya, D. N., and Sanides, F. 1973. Architectonic parcellation of the temporal operculum in rhesus monkey and its projection pattern. *Z. Anat. Entwicklungsgeschichte* **139:** 127–161.

Pantev, C., Hoke, M., Lehnertz, K., Lutkenhoner, B., Anogianakis, G., and Wittkowski, W. 1988. Tonotopic organization of the human auditory cortex revealed by transient auditory evoked magnetic fields. *Electroencephalogr. Clin. Neurophysiol.* **69:** 160–170.

Pantev, C., Hoke, M., Lutkenhoner, B., and Lehnertz, K. 1989. Tonotopic organization of the auditory cortex: Pitch versus frequency representation. *Science* **246:** 486–488.

Penhune, V. B., Zatorre, R. J., MacDonald, J. D., and Evans, A. C. 1996. Interhemispheric anatomical differences in human primary auditory cortex: Probabilistic mapping and volume measurement from magnetic resonance scans. *Cereb. Cortex* **6:** 661–672.

Rauschecker, J. P., and Tian, B. 2000. Mechanisms and streams for processing of "what" and "where" in auditory cortex. *Proc. Natl. Acad. Sci. USA* **97:** 11800–118006.

Rauschecker, J. P. 1997. Processing of complex sounds in the auditory cortex of cat, monkey, and man. *Acta Oto-Laryngol. Suppl.* **532:** 34–38.

Rauschecker, J. P., Tian, B., and Hauser, M. 1995. Processing of complex sounds in the macaque nonprimary auditory cortex. *Science* **268:** 111–114.

Rauschecker, J. P., Tian, B., Pons, T., and Mishkin, M. 1997. Serial and parallel processing in rhesus monkey auditory cortex. *J. Comp. Neurol.* **382:** 89–103.

Rivier, F., and Clarke, S. 1997. Cytochrome oxidase, acetylcholinesterase, and NADPH-diaphorase staining in human supratemporal and insular cortex: Evidence for multiple auditory areas. *NeuroImage* **6:** 288–304.

Romani, G. L., Williamson, S. J., and Kaufman, L. 1982. Tonotopic organization of the human auditory cortex. *Science* **216:** 1339–1340.

Romanski, L. M., Bates, J. F., and Goldman-Rakic, P. S. 1999. Auditory belt and parabelt projections to the prefrontal cortex in the rhesus monkey. *J. Comp. Neurol.* **403:** 141–157.

Scheich, H., Baumgart, F., Gaschler-Markefski, B., Tegeler, C., Tempelmann, C., Heinze, H. J., Schindler, F., and Stiller, D. 1998. Functional magnetic resonance imaging of a human auditory cortex area involved in foreground-background decomposition. *Eur. J. Neurosci.* **10:** 803–809.

Talairach, P., and Tournoux, J. 1988. *A Stereotactic Coplanar Atlas of the Human Brain*. Thieme, Stuttgart.

Talavage, T. M., Ledden, P. J., Benson, R. R., Rosen, B. R., and Melcher, J. R. 2000. Frequency-dependent responses exhibited by multiple regions in human auditory cortex. *Hearing Res.* **150:** 225–244.

Tian, B., Reser, D., Durham, A., Kustov, A., and Rauschecker, J. P. 2001. Functional specialization in rhesus monkey auditory cortex. *Science* **292:** 290–293.

Ugurbil, K., Garwood, M., Ellermann, J., Hendrich, K., Hinke, R., Hu, X., Kim, S. G., Menon, R., Merkle, H., and Ogawa, S. 1993. Imaging at high magnetic fields: Initial experiences at 4 T. *Magn. Reson. Q.* **9:** 259–277.

von Economo, C., and Koskinas, G. N. 1925. *Die Cytoarchitektonik der Hirnrinde.* Springer, Berlin.

Wessinger, C. M., Bounocore, M. H., Kussmaul, C. L., and Mangun, G. R. 1997. Tonotopy in human auditory cortex examined with functional magnetic resonance imaging. *Hum. Brain Mapp.* **5:** 18–25.

Wessinger, C. M., VanMeter, J., Tian, B., Van Lare, J., Pekar, J., and Rauschecker, J. P. 2001. Hierarchical organization of the human auditory cortex revealed by functional magnetic resonance imaging. *J. Cogn. Neurosci.* **13:** 1–7.

Woldorff, M. G., Gallen, C. C., Hampson, S. A., Hillyard, S. A., Pantev, C., Sobel, D., and Bloom, F. E. 1993. Modulation of early sensory processing in human auditory cortex during auditory selective attention. *Proc. Natl. Acad. Sci. USA* **90:** 8722–8726.

Worsley, K. J., and Friston, K. J. 1995. Analysis of fMRI time-series revisited—Again. [letter; comment]. *NeuroImage* **2:** 173–181.